CrYogenic Brightness-Optimized Radiofrequency Gun (CYBORG) Test Bed

Gerard Lawler[1], Fabio Bosco[2], Obed Camacho[1], Atsushi Fukusawa[1], Zenghai Li[3], Nathan Majernik[1], Pratik Manwani[1], Andrea Mostacci[2], Jake Parsons[1], Yusuke Sakai[1], Evgenya Simakov[4], Bruno Spataro[5], Sami Tantawi[3], Tsuyoshi Tajima[4], Oliver Williams[1], and James Rosenzweig[1]

[1] UCLA, Los Angeles, CA 90095

[2] Sapienza University of Rome, Rome, Italy 00185

[3] SLAC, Menlo Park, CA, 94025

[4] LANL, Los Alamos, NM 87545

[5] INFN-LNF, Frascati, Italy 00044

Outline of presentation

1. Background & Motivations
2. Cryogenic photoemission
3. CYBORG Design
4. Fabrication & Commissioning Status
5. Future Steps
6. Conclusions

1. Background

- Significant focus photoinjector; wakefield; fundamental high field physics
- TopGun previous development in Sband
- Based on normal conducting cryogenic gradient improvements which we can

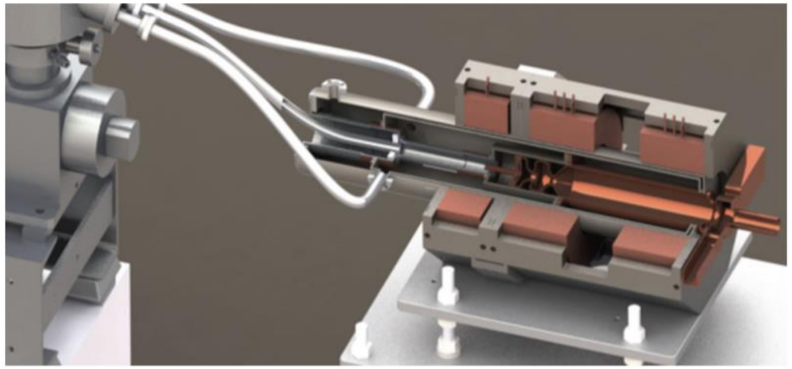

$$P \sim f_{rf}^{-2}$$

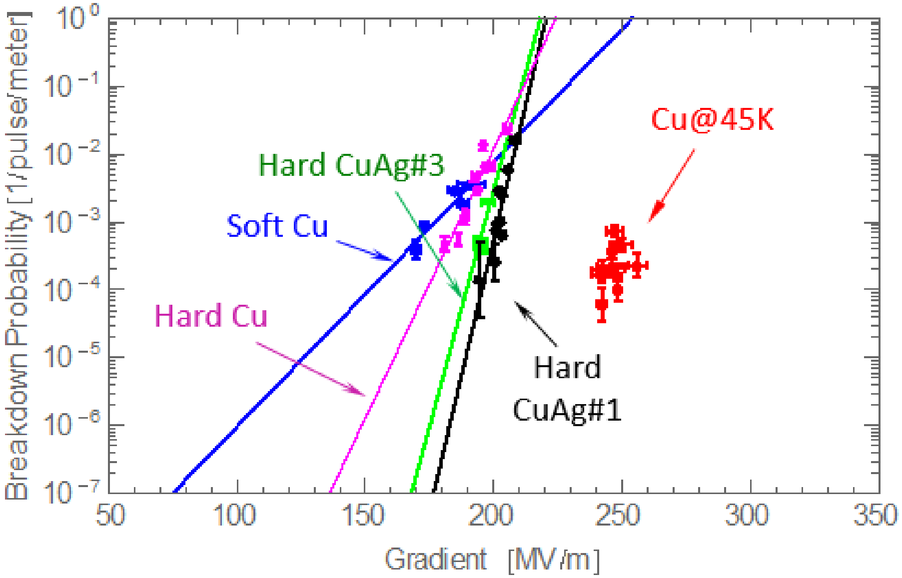

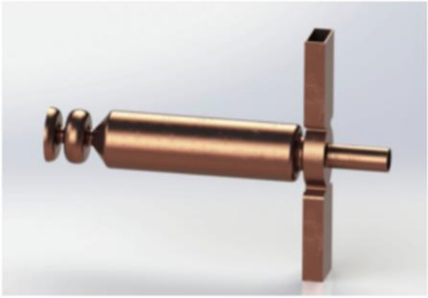

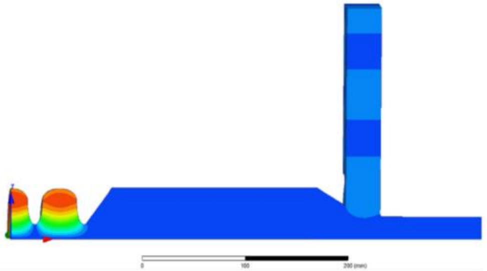

J. B. Rosenzweig et al., Phys. Rev. Accel. Beams, vol. 22, p. 023 403, 2 Feb. 2019. doi: 10.1103/PhysRevAccelBeams.22.023403

1. Motivational Cases

- Ultra-compact xray free electron laser (UCXFEL) concept dependent on cryo-enabled high gradients and distributed coupling RF design
  - Reduction of detrimental breakdown
- Photoinjector and associated brightness improvements most relevant but linac sections also implications for longer machines
  - Cool Copper Collider (C^3) (below)
- Cathodes studies of interest for NSF CBB

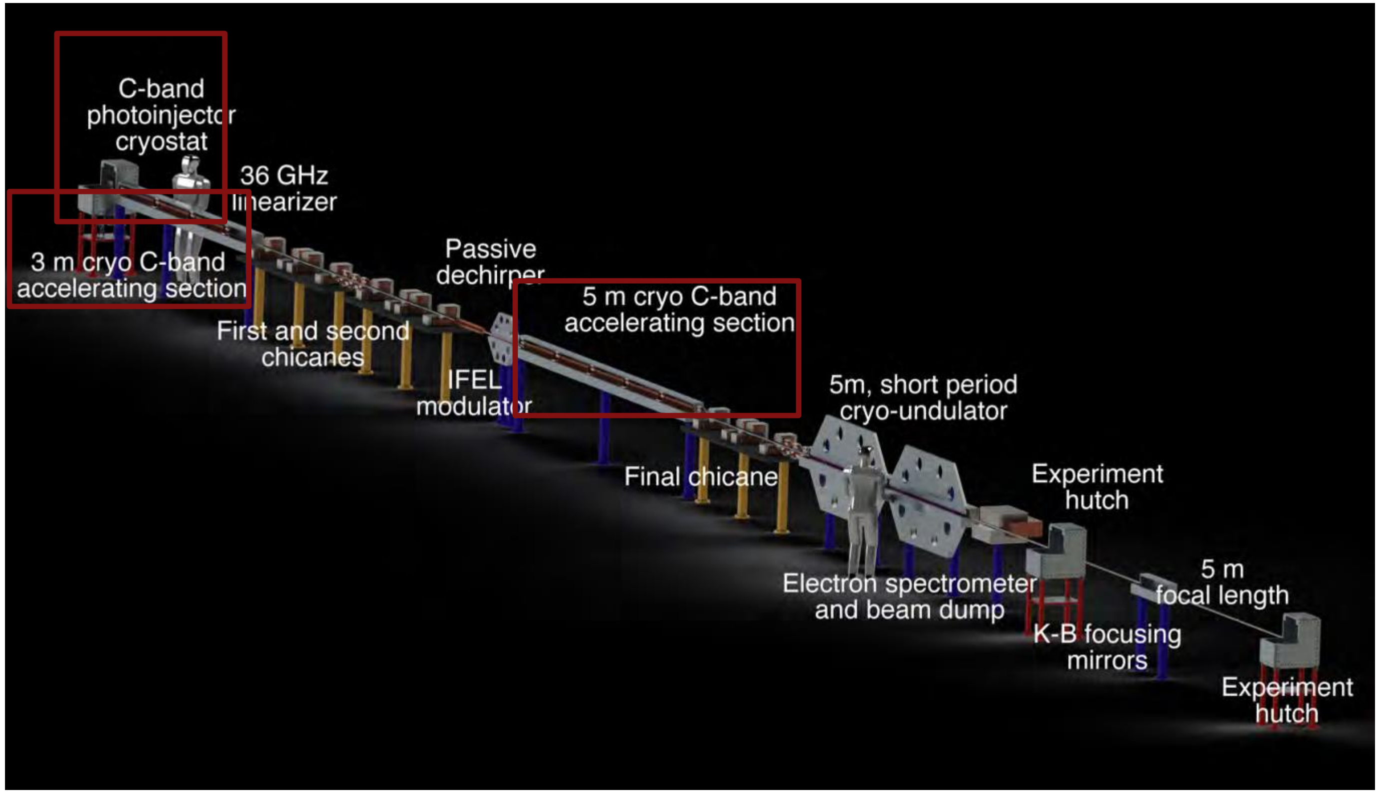

J. B. Rosenzweig et al., New J. Phys., vol. 22, p. 093 067, Sep. 2020. doi: 10.1088/1367-2630/abb16.

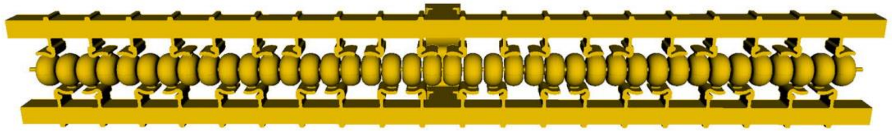

1. Additional CYBORG Functions

- Cavity fabrication & structure test
- Infrastructure development

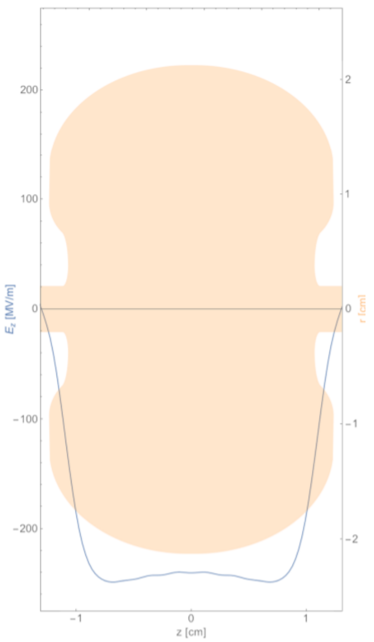

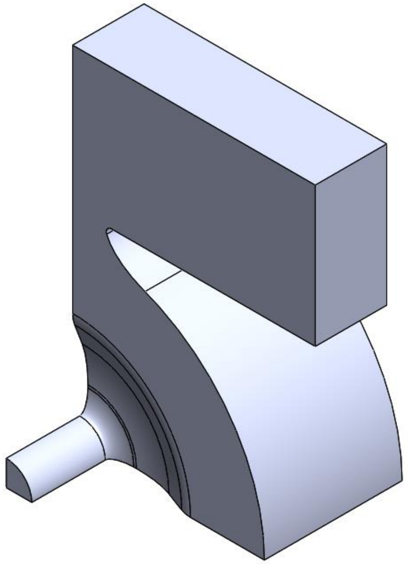

R. R. Robles et al., Phys. Rev. Accel. Beams, vol. 24, p. 063 401, 6 Jun. 2021. doi: `10.1103/PhysRevAccelBeams.24.063401`.

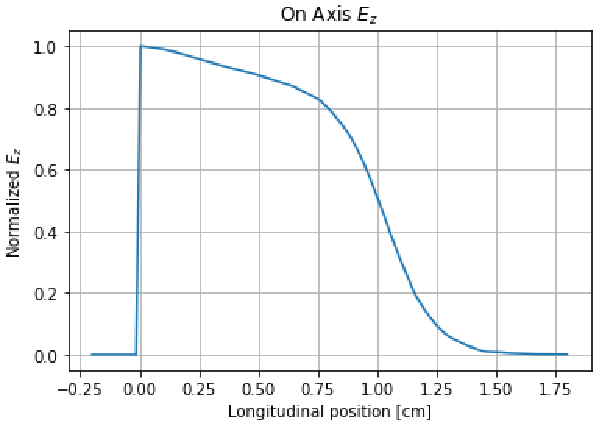

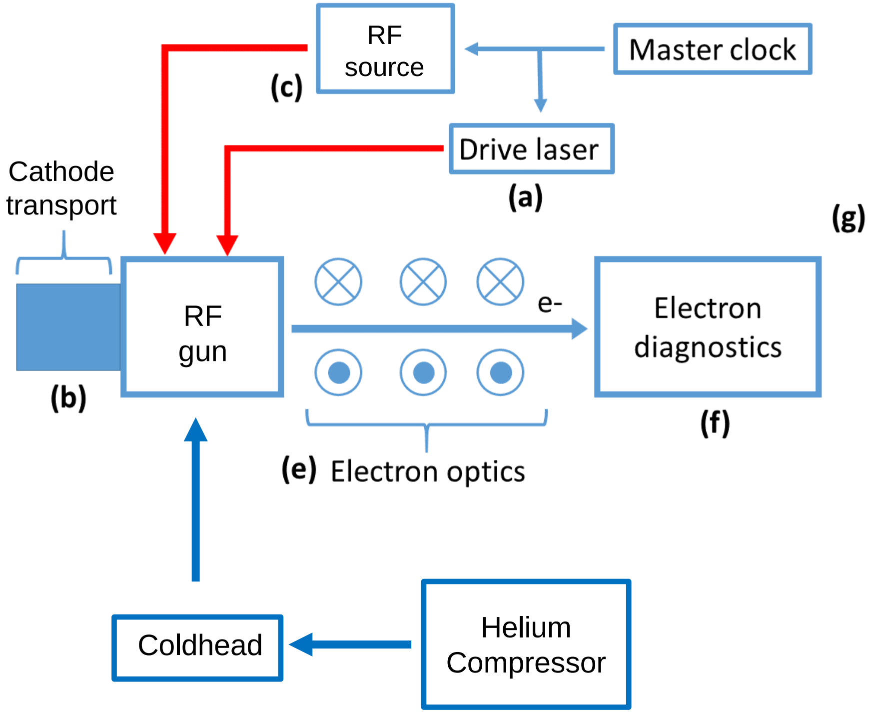

2. Metallic photoemission

- Emission properties of photocathodes change @ cryogenic temperatures (<93K)
- Where hν ≫ ϕeff scaling as below

$$k_b T_c = (h\nu - \phi_{\text{eff}})/3$$

$$QE = N_{e-}/N_\gamma \propto (h\nu - \phi_{\text{eff}})^2$$

- Cu photocathodes emission temp ranges from ~100 meV to 1 eV depending on wavelength
- 1D brightness scaling (below)
- From UXFEL NJP, note 6D brightness importance

$$B_{e,b} \approx \frac{2ec\varepsilon_0}{k_B T_c}\left(E_0 \sin\phi_0\right)^2$$

D. Dowell and J. Schmerge, Phys. Rev. ST Accel. Beams 12, 074201 (2009).

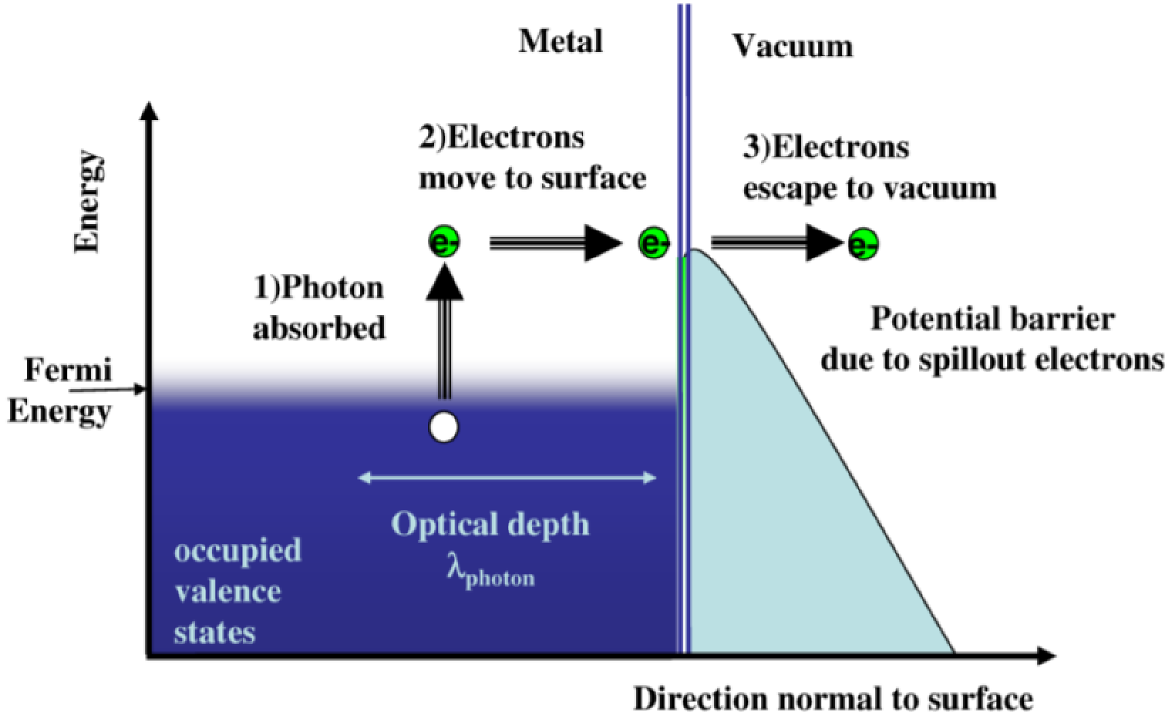

2. Cryogenic metallic photoemission

- Near threshold emission from tail of Fermi-Dirac distribution
- Now including full FD distribution with temperature dependence (right)
- hv → ϕeff, photoemission temperature approaches physical cathode temperature, k_BT_c → 26 meV at 300 K
- Very low QE

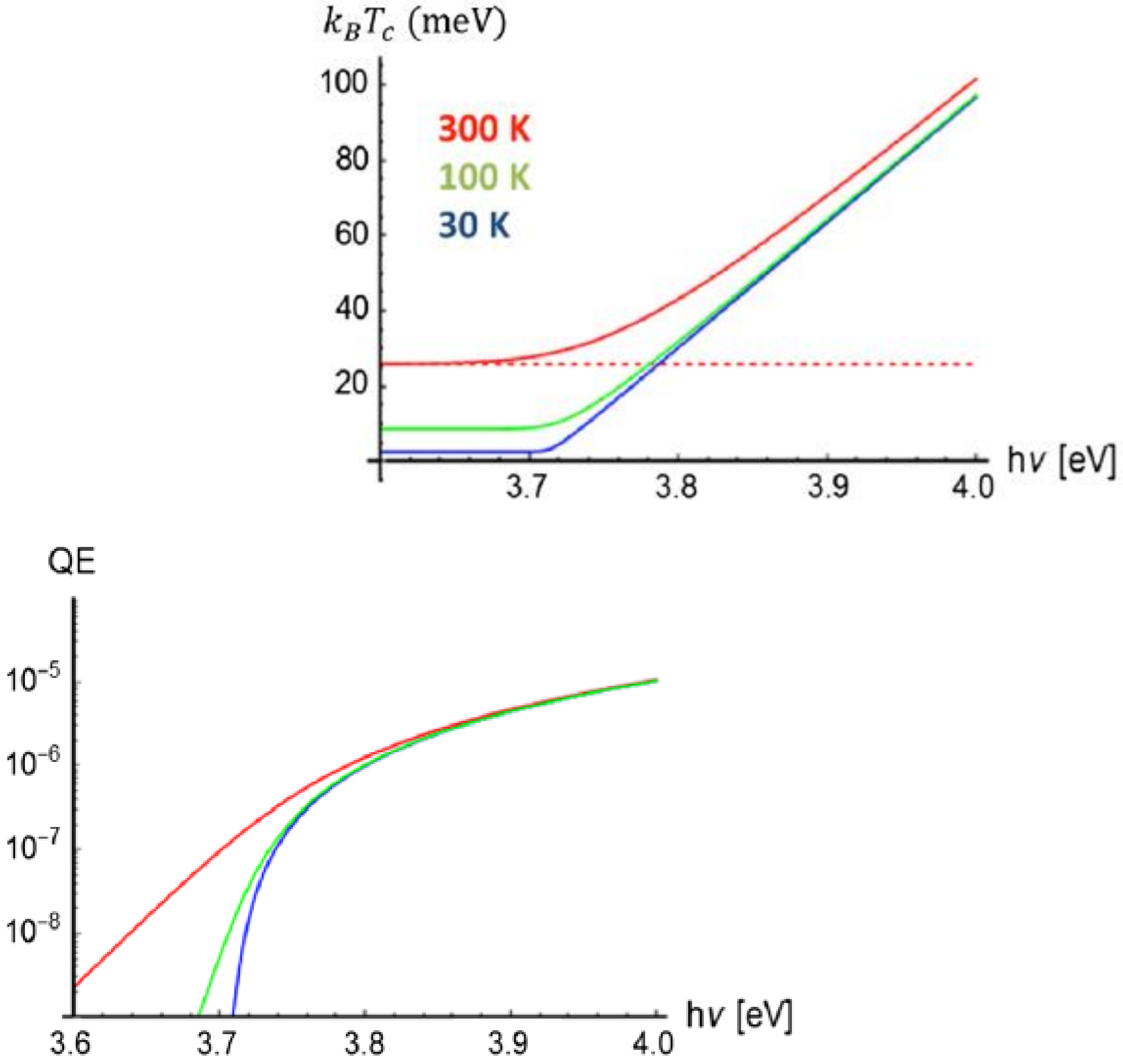

2. Cryogenic metallic cathode issues

- Easiest if Cu satisfies all cathode requirements
- 100 pC from 75 um rms spot size at 250 MV/m accelerating field, 38 nm-rad intrinsic emittance ➔ 130 meV MTE, ~10^{12} e^-/cm^2
- Extremely challenging due to non-linear emission
- 50 fs pulse – could be better for 5 ps pulse
- Need to characterize cathodes in these extreme condition

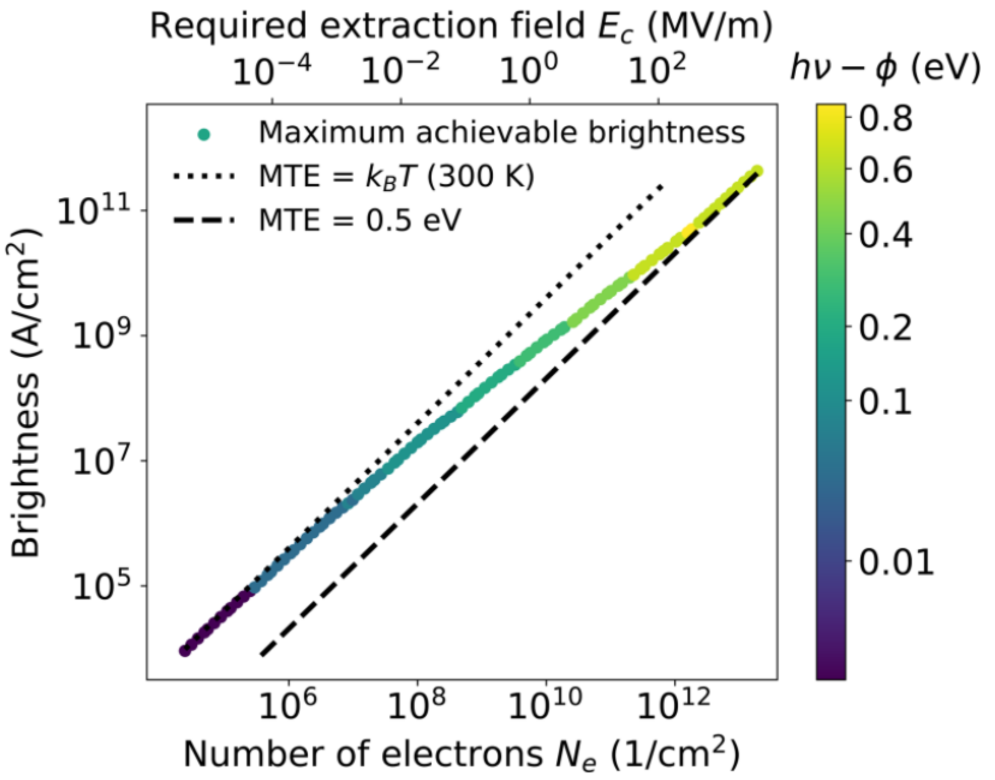

J. K. Bae, I. Bazarov, P. Musumeci, S. Karkare, H. Padmore, and J. Maxson, J. Appl. Phys. 124, 244903 (2018).

2. Cryogenic semiconductor cathodes

- High QE photocathode, many orders of magnitude higher than Cu, promising
- Alkali antimonides, Cs2Te
  - Field emission could be an issue due to lower work functions/roughness.
- Cs/GaN or n-doped polar GaN
  - High QE in UV, high work function
  - Could result in very low MTE
  - never been tested in photoinjectors
  - Potential vacuum concerns
- Reduction of MTE at cryogenic temps observed

NaKSb

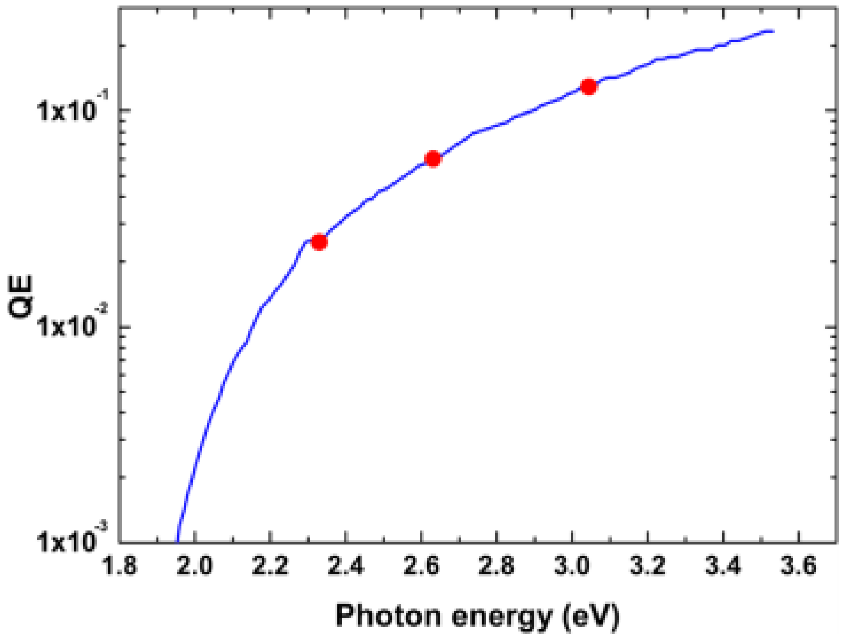

L. Cultrera et al., Appl. Phys. Lett. 103, 103504 (2013).

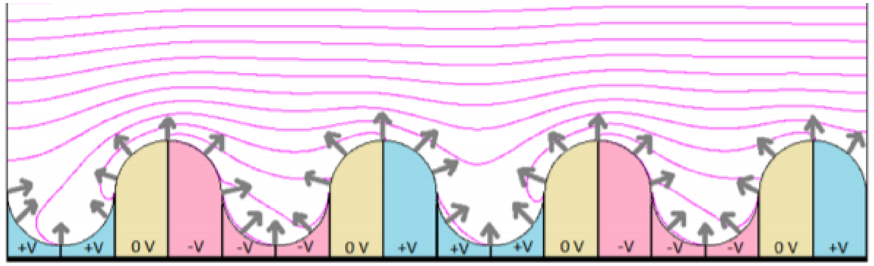

G. S. Gevorkyan et al., Phys. Rev. Accel. Beams, vol. 21,p. 093 401, 9 Sep. 2018.

3. CYBORG w/ diagnostics

- Simplified phase 1 of cryogenic test bed design
- Measurements of QE for cryogenic copper

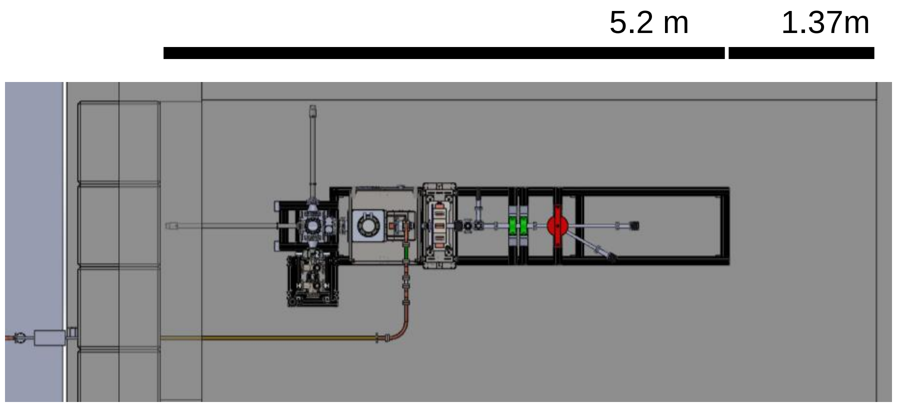

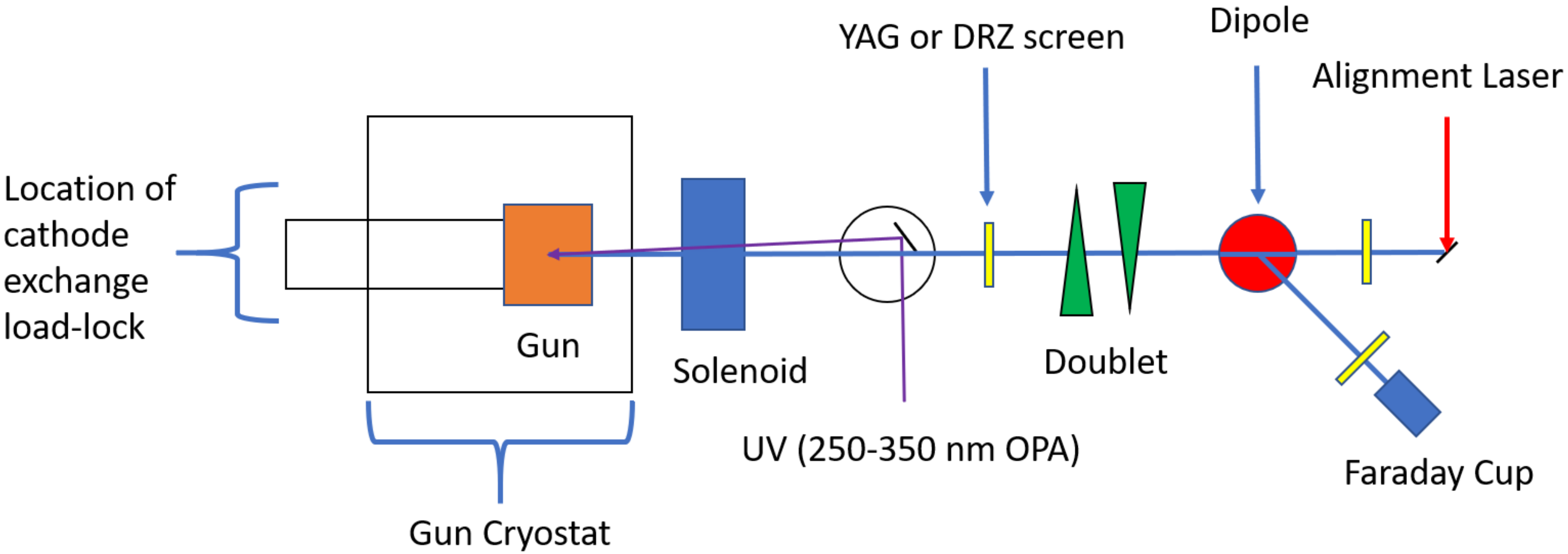

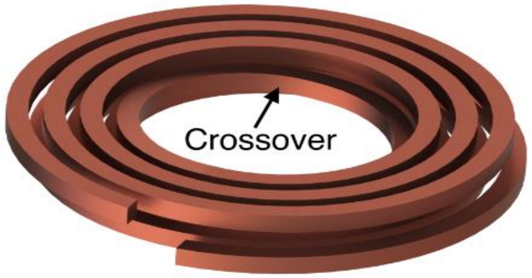

N. Majernik, A. Fukasawa, J. B. Rosenzweig, and A. Suraj, presented at the 12th Int. Particle Accelerator Conf. (IPAC'21), Campinas, Brazil, May 2021, paper TUPAB094

3. Cathode Diagnostic Beamline

- Load lock with phase2 diagnostic suite: TEM grid currently in simulation phase; additional solenoid; additional quad to make triplet
- Overview below with CAD smaller inset

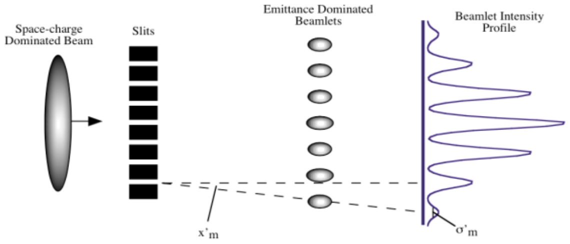

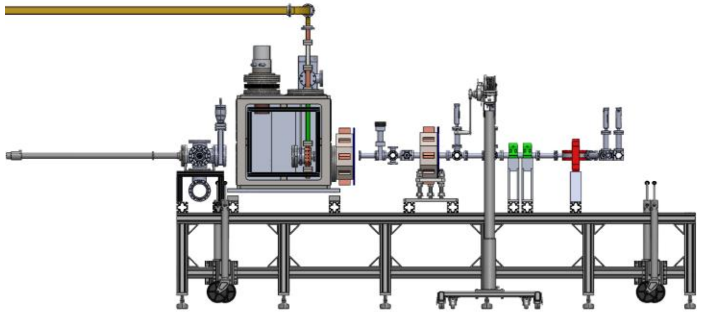

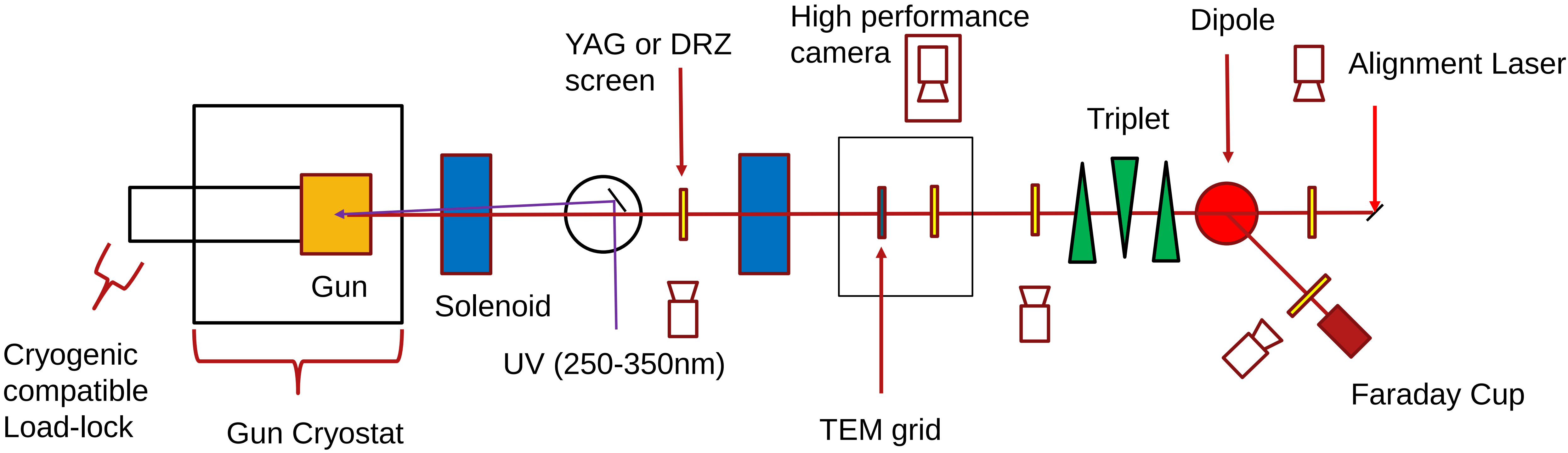

D. Marx et al. Phys. Rev. Accel. Beams 21, 102802 (2018).

3. MOTHRA Lab

- Multi-Option Testing of High-field Radiofrequency Accelerators (MOTHRA)
- Suitable for cryogenics testing; C-band infrastructure development; low energy (single MeV) beamline for cathode studies

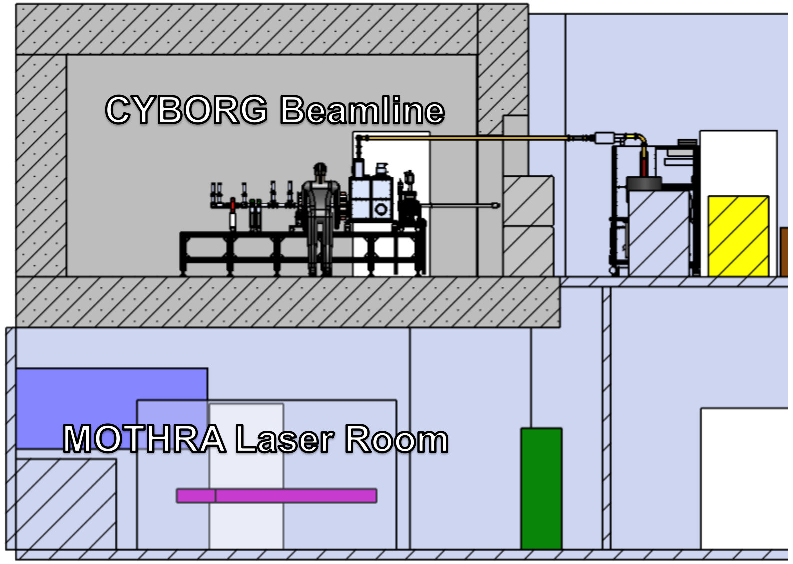

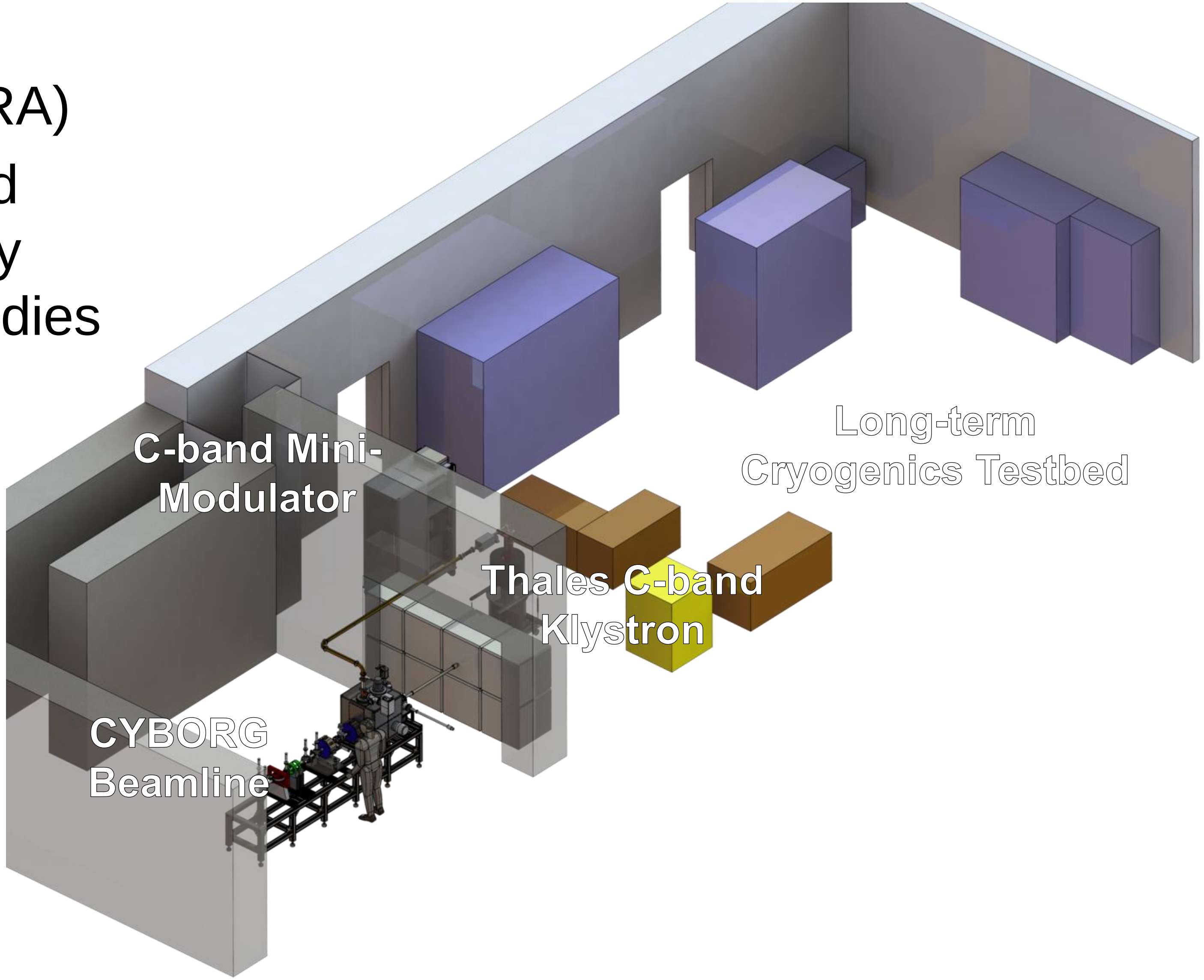

3. MOTHRA Lab

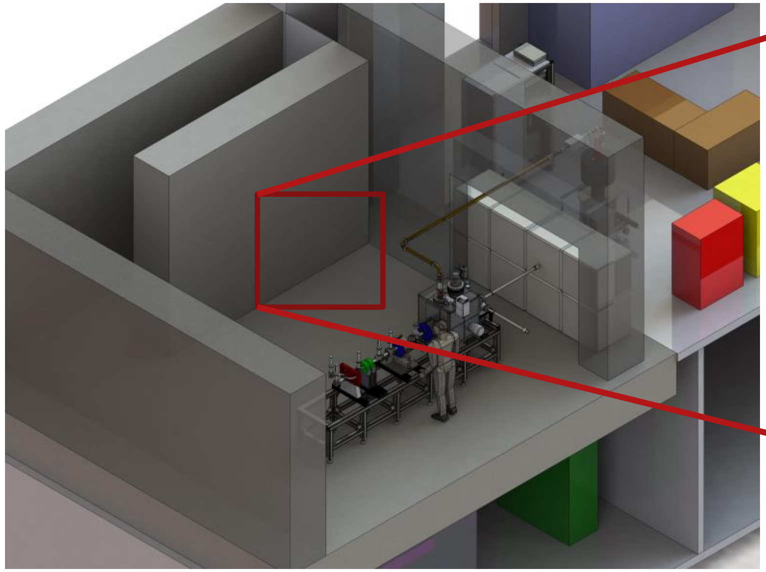

- Cryogenic cooling system development setup (cryostat v1, left)
- Conduction cooling setup for cost effectiveness and future miniaturization concerns

- C-band modulator construction (right)

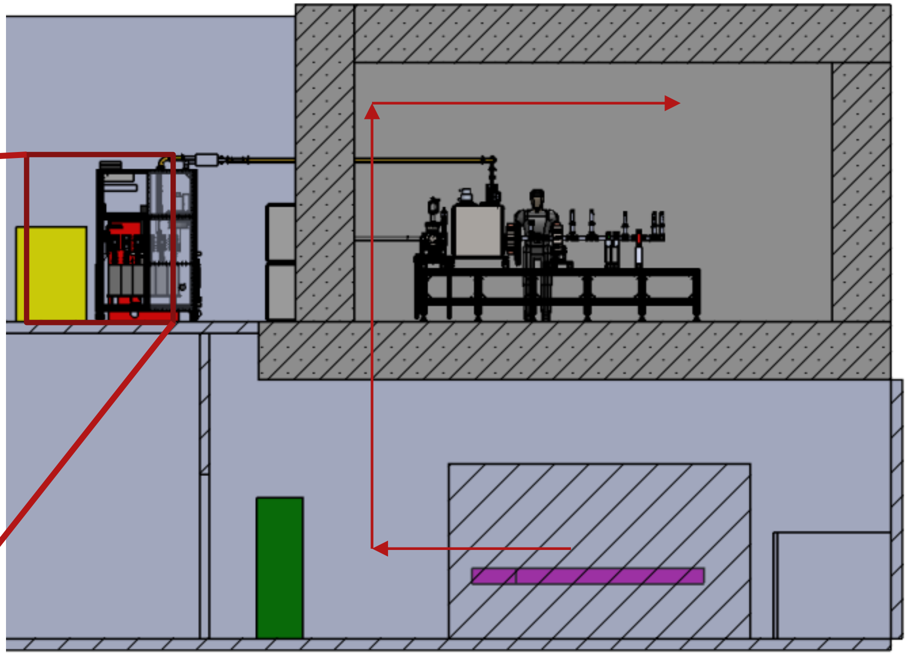

3. MOTHRA Lab

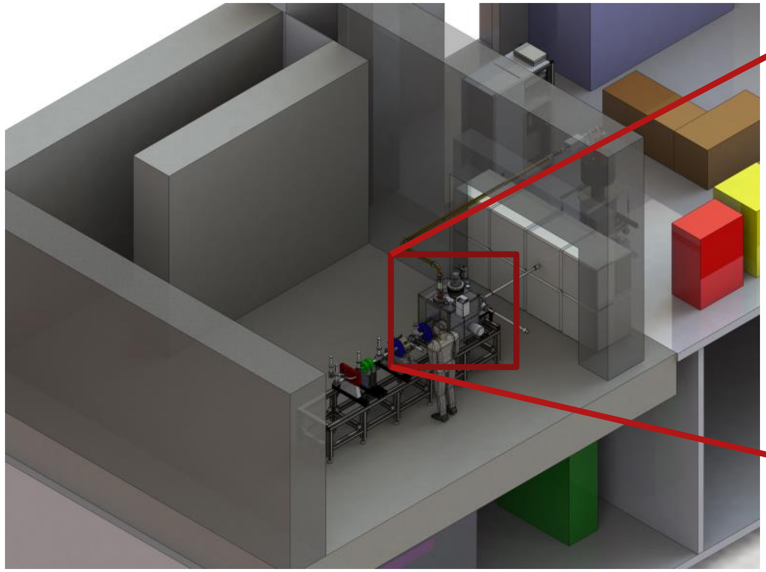

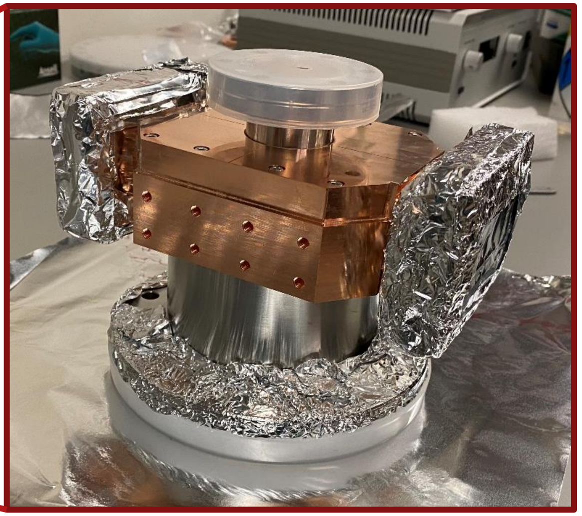

- Cryogenic cathode diagnostic test bed
- Using load lock-enabled ½ cell high gradient photogun (CYBORG, left)

- Clean room for UV production using legacy SLAC GTF setup

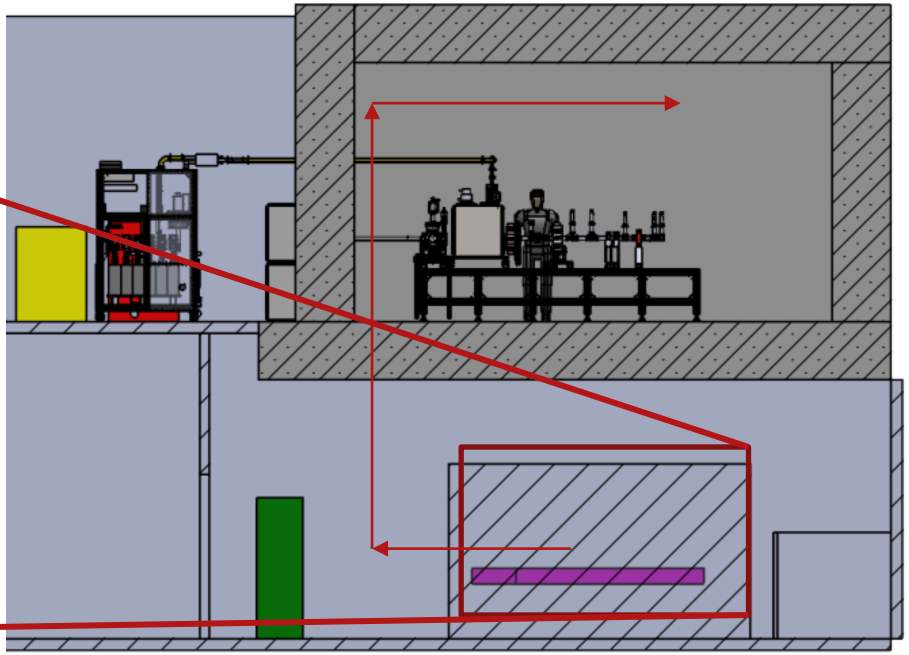

3. RF Design Parameters

- Reentrant cavity with high shunt impedance
- Peak electric field around cathode surface

E field magnitude

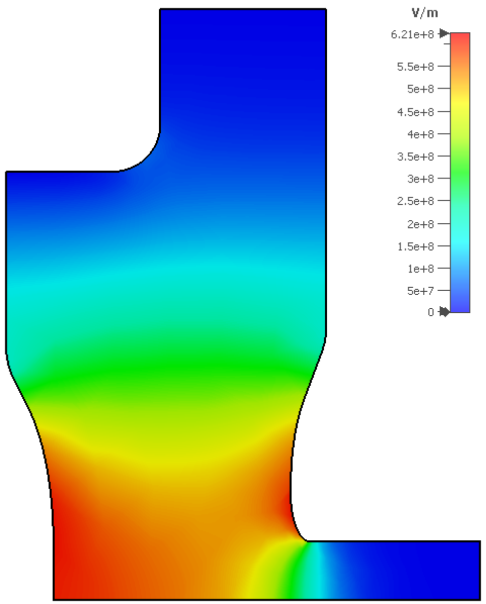

H field magnitude

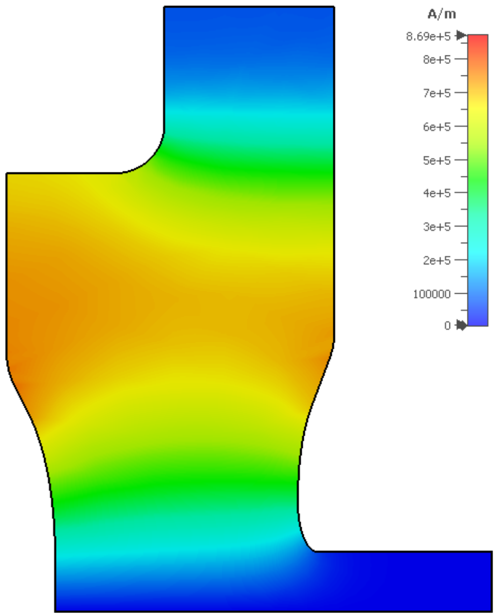

Parameter	295K	77K	45K
Launch field	-	120 MV/m	120 MV/m
Frequency	5.695 GHz	5.712 GHz	5.713 GHz
β	0.7	4	5.3
Q0	8579	23000	38000
Filling time	-	0.26 us	0.3 us
RF Power requirement	-	0.52 MW	0.48 MW
Energy deposition	-	0.17 J/pulse	0.1 J/pulse

G. Lawler et al., in Proc. IPAC'22, JACoW Publishing, Geneva, Switzerland, Jul. 2022, pp. 2544–2547, isbn: 978-3-95450-227-1. doi: 10.18429/JACoW-IPAC2022-THPOST046.

3. RF Design Parameters

- Reentrant cavity with high shunt impedance
- Peak electric field around cathode surface

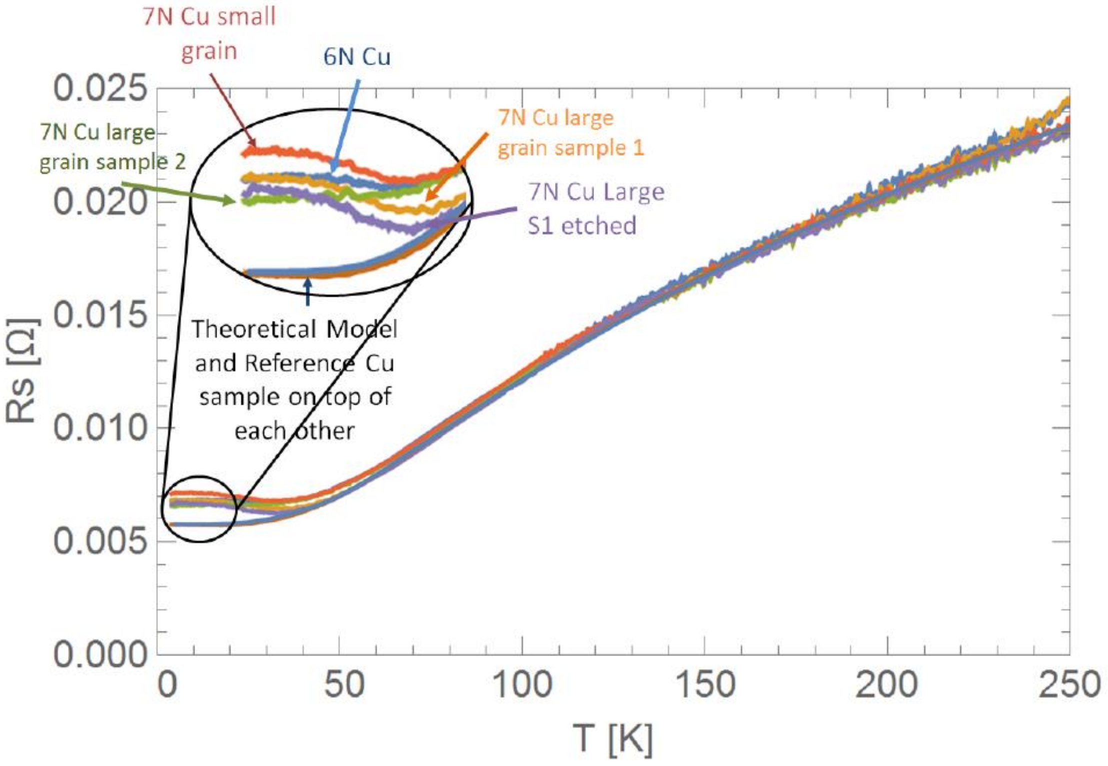

Parameter	295K	77K	45K
Launch field	-	120 MV/m	120 MV/m
Frequency	5.695 GHz	5.712 GHz	5.713 GHz
β	0.7	4	5.3
Q0	8579	23000	38000
Filling time	-	0.26 us	0.3 us
RF Power requirement	-	0.52 MW	0.48 MW
Energy deposition	-	0.17 J/pulse	0.1 J/pulse

G. Lawler et al., in Proc. IPAC'22, JACoW Publishing, Geneva, Switzerland, Jul. 2022, pp. 2544–2547, isbn: 978-3-95450-227-1. doi: 10.18429/JACoW-IPAC2022-THPOST046.

3. RF Design Parameters

- Reentrant cavity with high shunt impedance
- Peak electric field around cathode surface

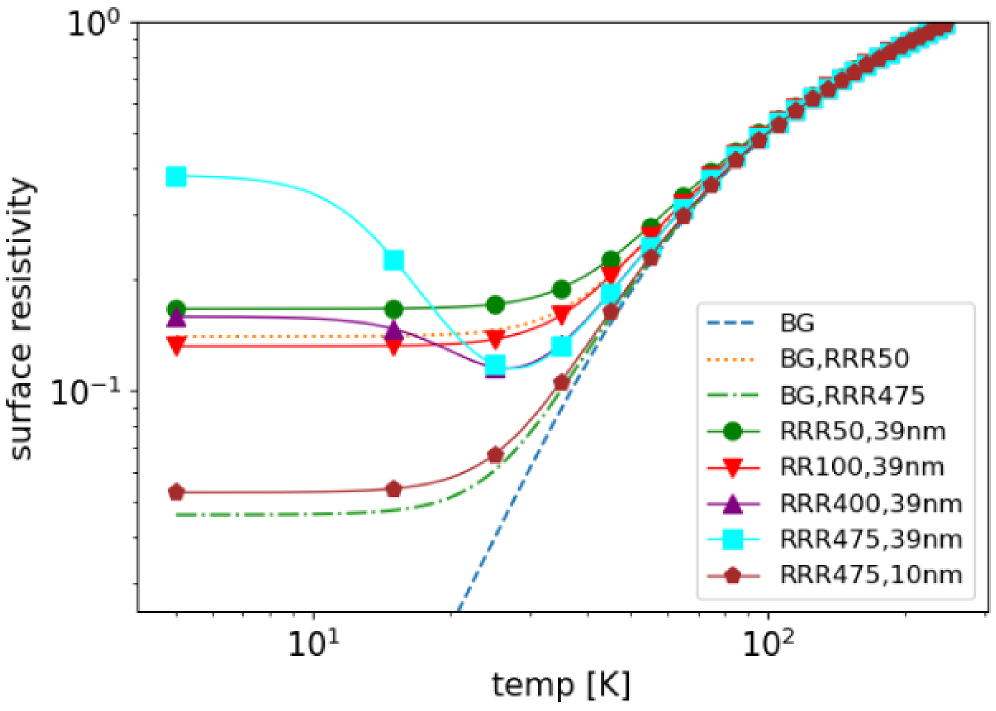

G. Lawler, A. Fukasawa, N. Majernik, and J. Rosenzweig, in Proc. IPAC'22, JACoW Publishing, Geneva, Switzerland, Jul. 2022, pp. 2540–2543, isbn: 978-3-95450-227-1. doi: 10.18429/JACoW-IPAC2022-THPOST045.

Parameter	295K	77K	45K
Launch field	-	120 MV/m	120 MV/m
Frequency	5.695 GHz	5.712 GHz	5.713 GHz
β	0.7	4	5.3
Q0	8579	23000	38000
Filling time	-	0.26 us	0.3 us
RF Power requirement	-	0.52 MW	0.48 MW
Energy deposition	-	0.17 J/pulse	0.1 J/pulse

G. Lawler et al., in Proc. IPAC'22, JACoW Publishing, Geneva, Switzerland, Jul. 2022, pp. 2544–2547, isbn: 978-3-95450-227-1. doi: 10.18429/JACoW-IPAC2022-THPOST046.

3. Cathode Interface

- Forward compatibility needed for INFN style mini puck, etc.
- For phase 1 of test bed, CF flange sealed off w/ blank from back of cavity and test copper cathode

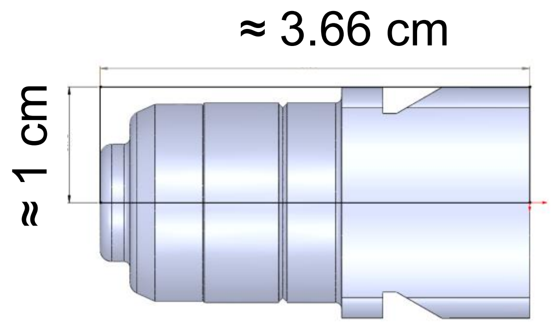

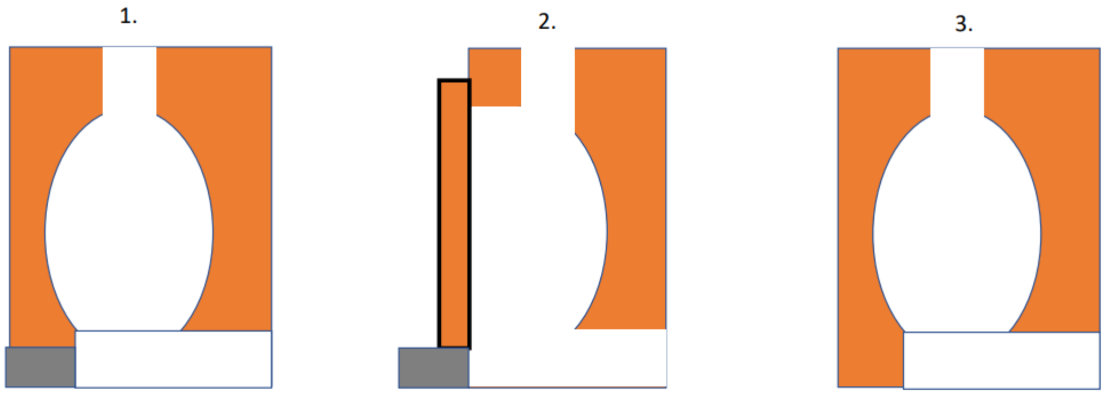

- Plug directly into cavity
- Useful for 1.6 cell to max gradient

- Good for cathode tests
- High gradient (120 MV/m) but lower than plug alone

- No cathode exchange
- Highest achievable gradients

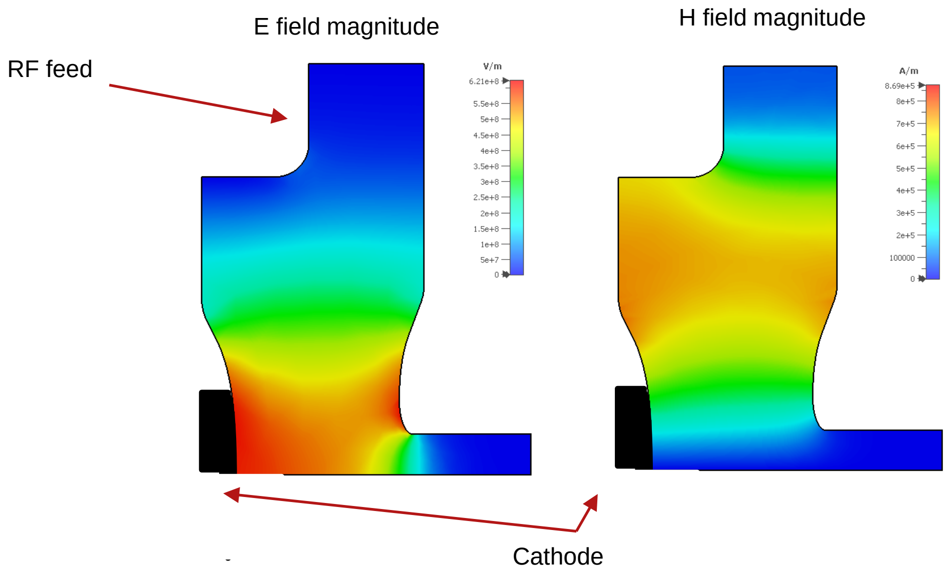

4. CAD

- CAD drawings
- Split seam brazing location necessitated by cavity machining tolerance requirements
- External features for alignment

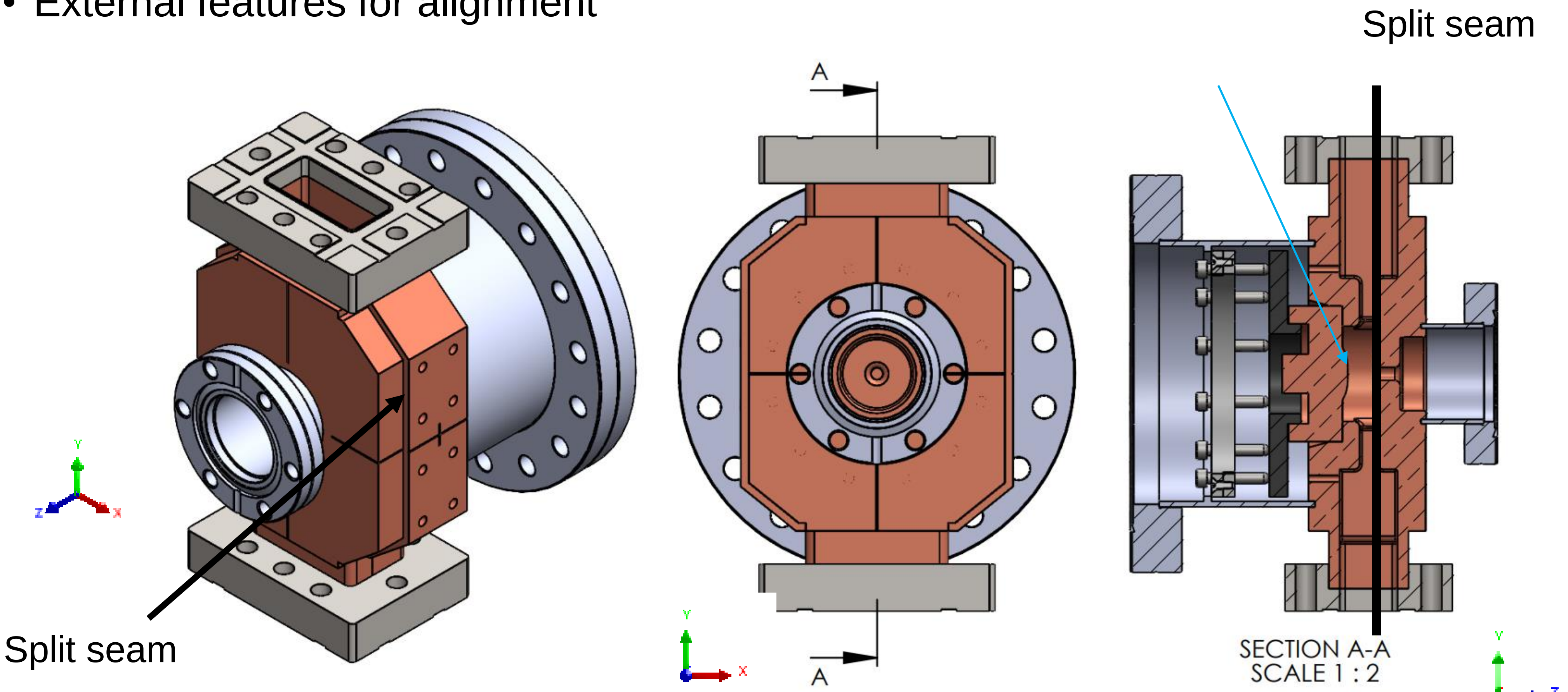

4. CAD Photos

- Cathode backplane press fit to begin
- Functional at Elettra lab in Trieste, Italy for FERMI seeded FEL
  - Uses high gradient BNL/SLAC/UCLA 1.6 cell electron gun
- Slow exchange not intended for final cathode testing but allows versatility with respect to cathode load lock integration

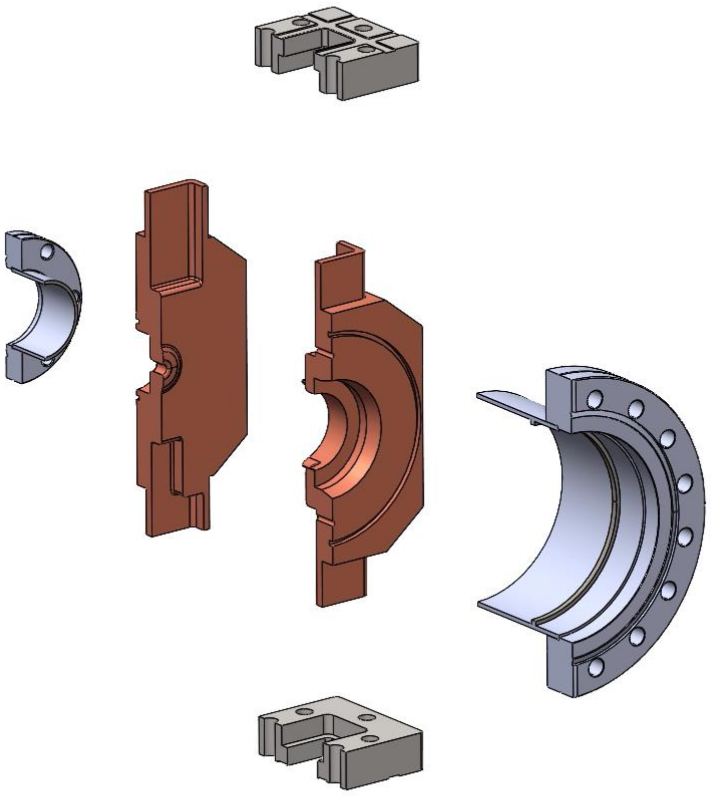

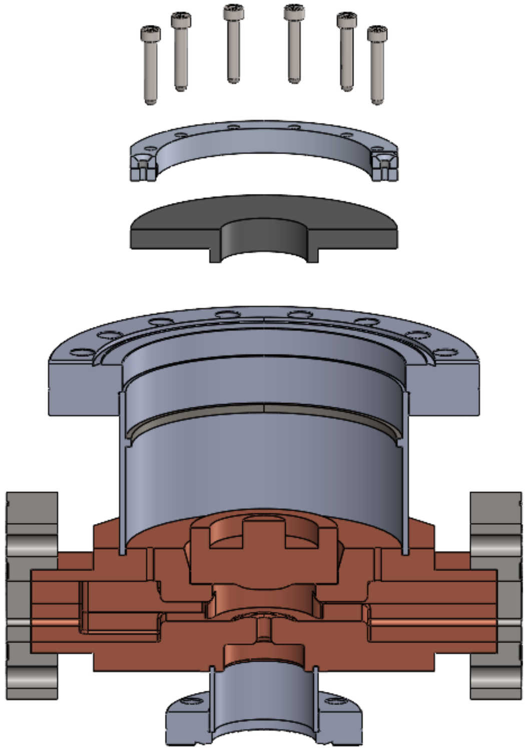

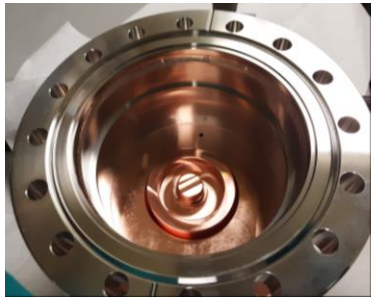

4. Steady State Thermal Sim

- Steady state thermal simulation results w/ 15W cooling from press fit with 3W heat leak budget

Description	Materials	Equivalent Area	Equivalent Power @ 65K	Equivalent Power @ 45K
Downstream CF flange	stainless, edge welded bellows	85 mm^2	4.8 W	5.2 W
Waveguide	Stainless	588 mm^2	6.6 W	7.1 W
Supports	Stainless + 2" G10	TBD	0.6 W	0.8 W
Diagnostic probes	Copper wiring	1.6 mm^2	≈ 0.1 W	≈ 0.1 W
Radiation	-	25000 mm^2	< 0.1 W	< 0.1 W
Pumping on dummy side	TBD	TBD	TBD	TBD
Upstream load lock	TBD	TBD	TBD	TBD
1Hz pulse heating	-	TBD	≈ 0.1 W	≈ 0.1 W

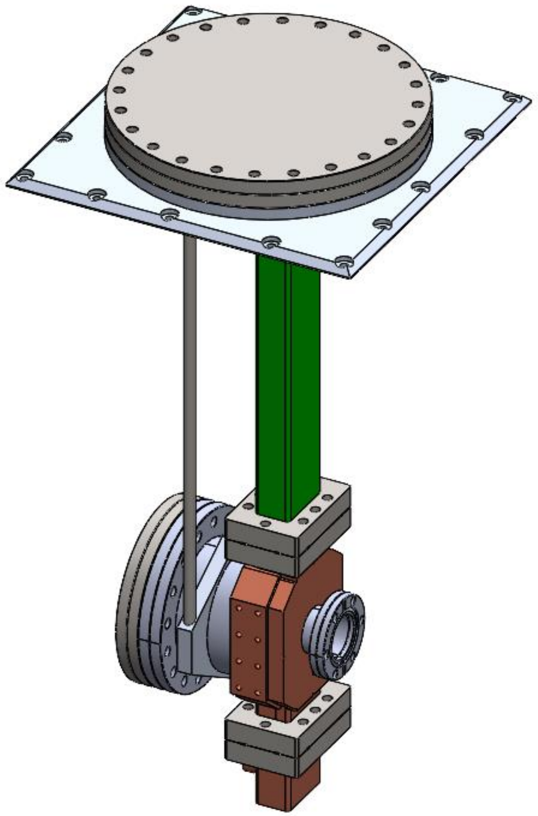

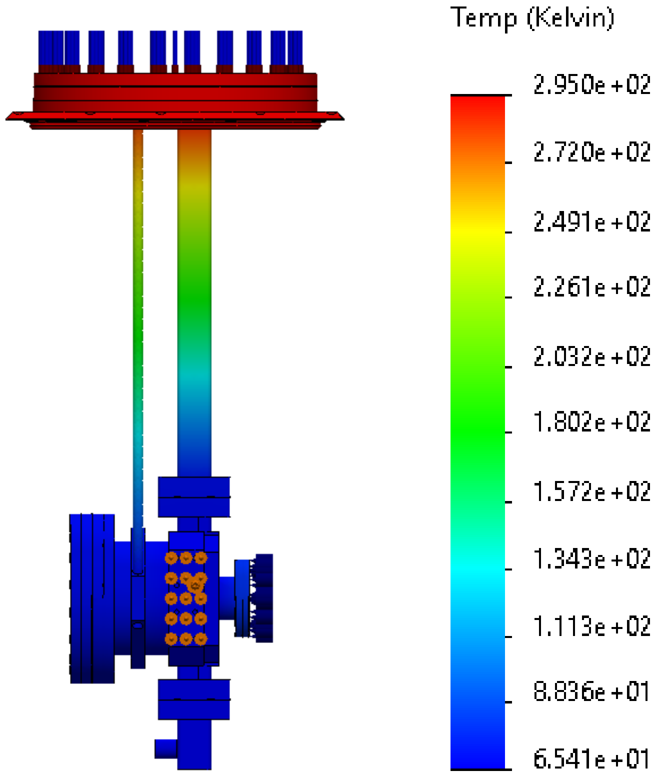

- Steady state thermal simulation results w/ 15W cooling from press fit with 3W heat leak budget

Description	Materials	Equivalent Area	Equivalent Power @ 65K	Equivalent Power @ 45K
Downstream CF flange	stainless, edge welded bellows	85 mm^2	4.8 W	5.2 W
Waveguide	Stainless	588 mm^2	6.6 W	7.1 W
Supports	Stainless + 2" G10	TBD	0.6 W	0.8 W
Diagnostic probes	Copper wiring	1.6 mm^2	≈ 0.1 W	≈ 0.1 W
Radiation	-	25000 mm^2	< 0.1 W	< 0.1 W
Pumping on dummy side	TBD	TBD	TBD	TBD
Upstream load lock	TBD	TBD	TBD	TBD
1Hz pulse heating	-	TBD	≈ 0.1 W	≈ 0.1 W

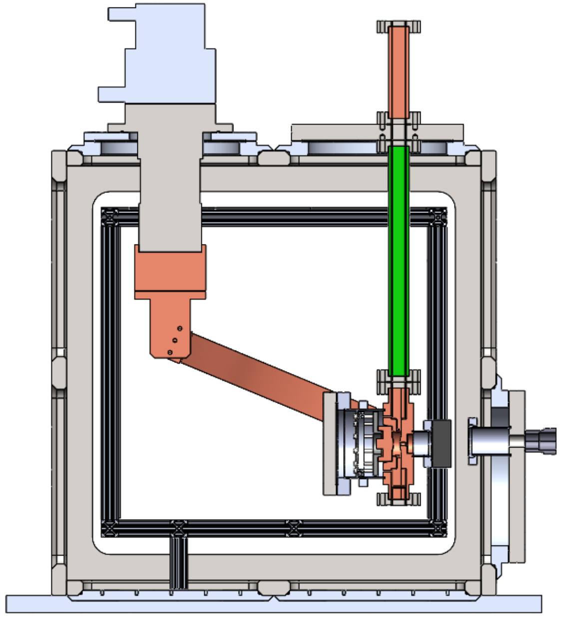

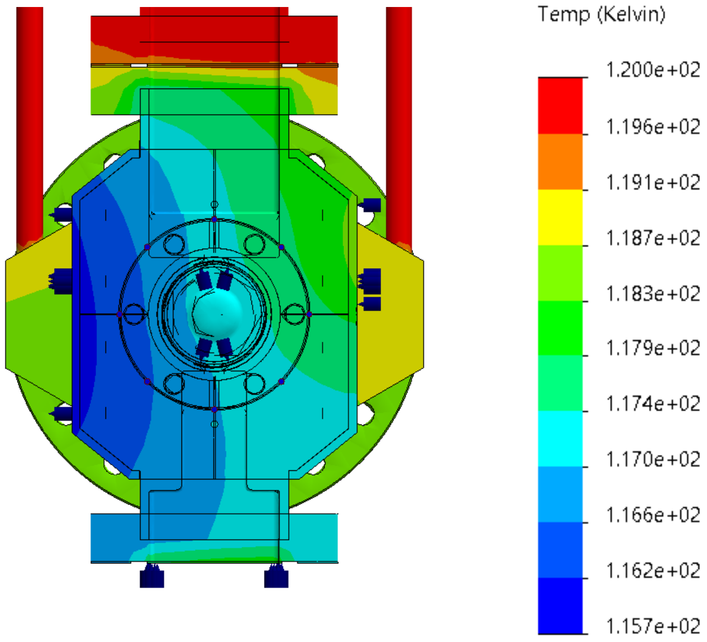

4. Cavity faces

Vacuum Venting ports

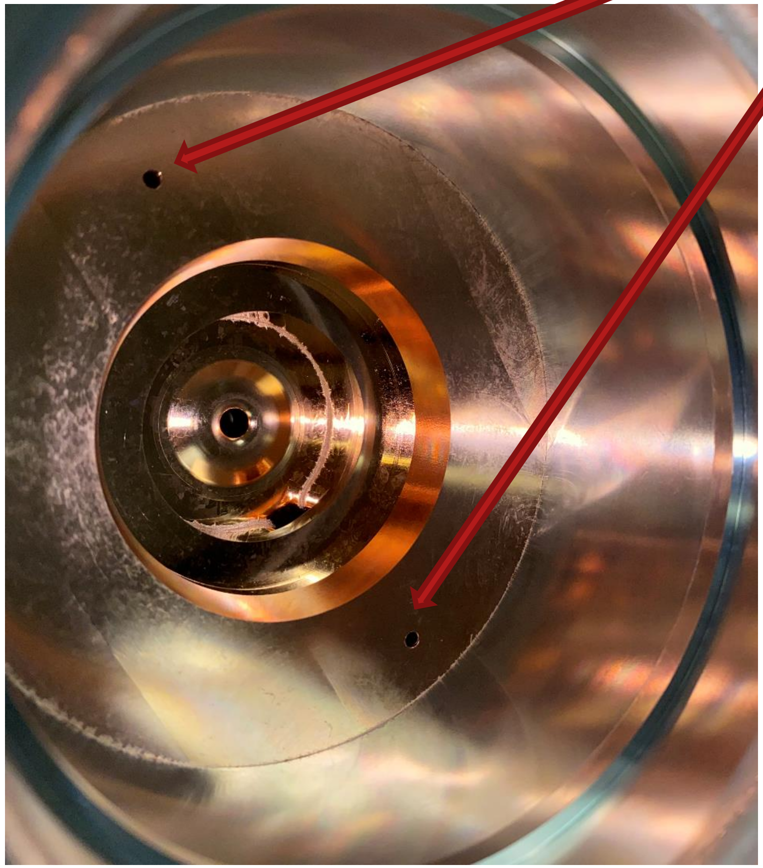

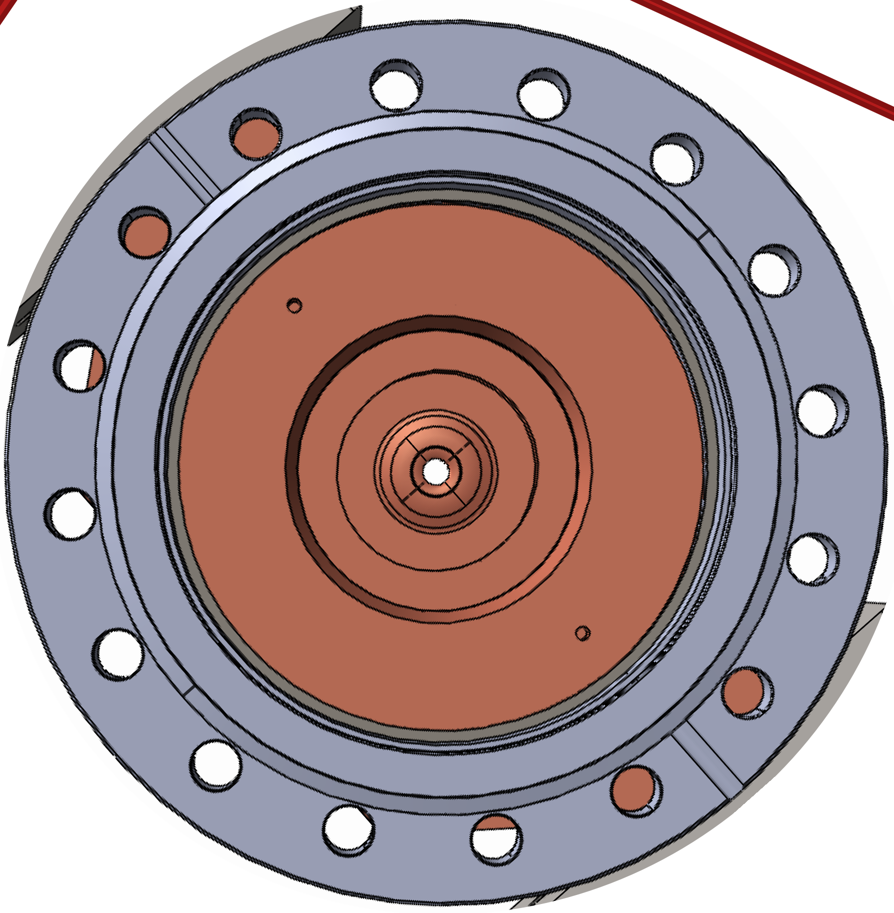

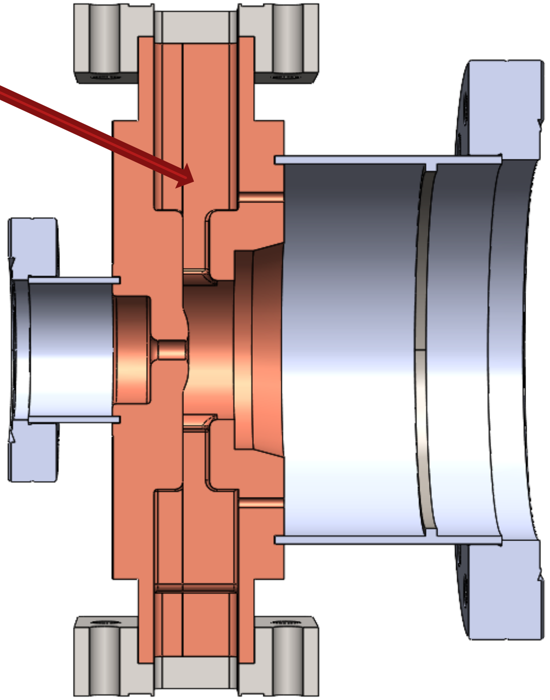

4. Cavity faces

- Circumference of front plane of ½ cell cavity

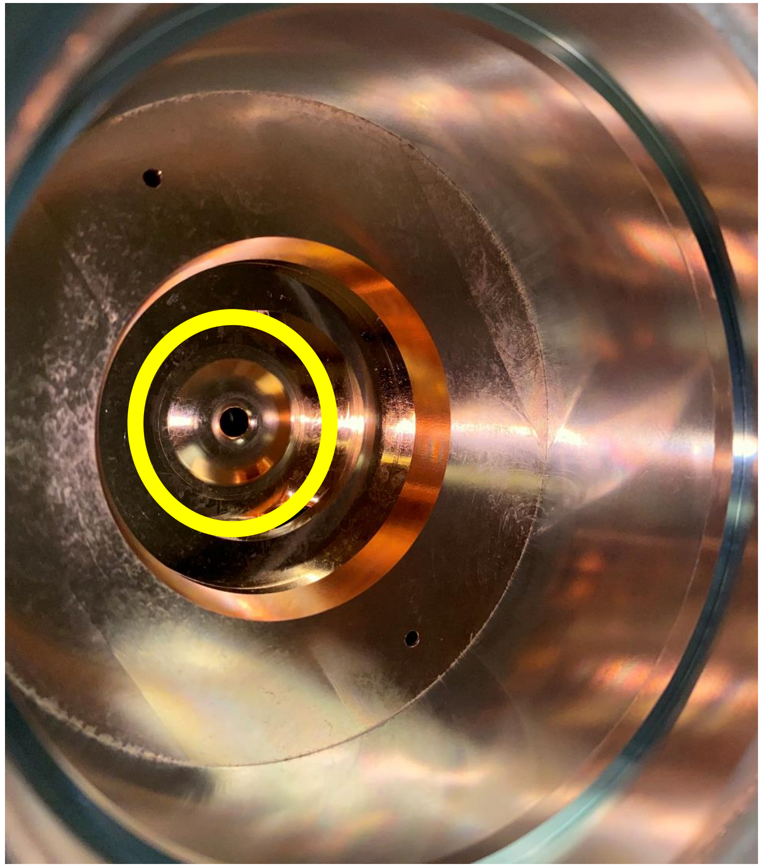

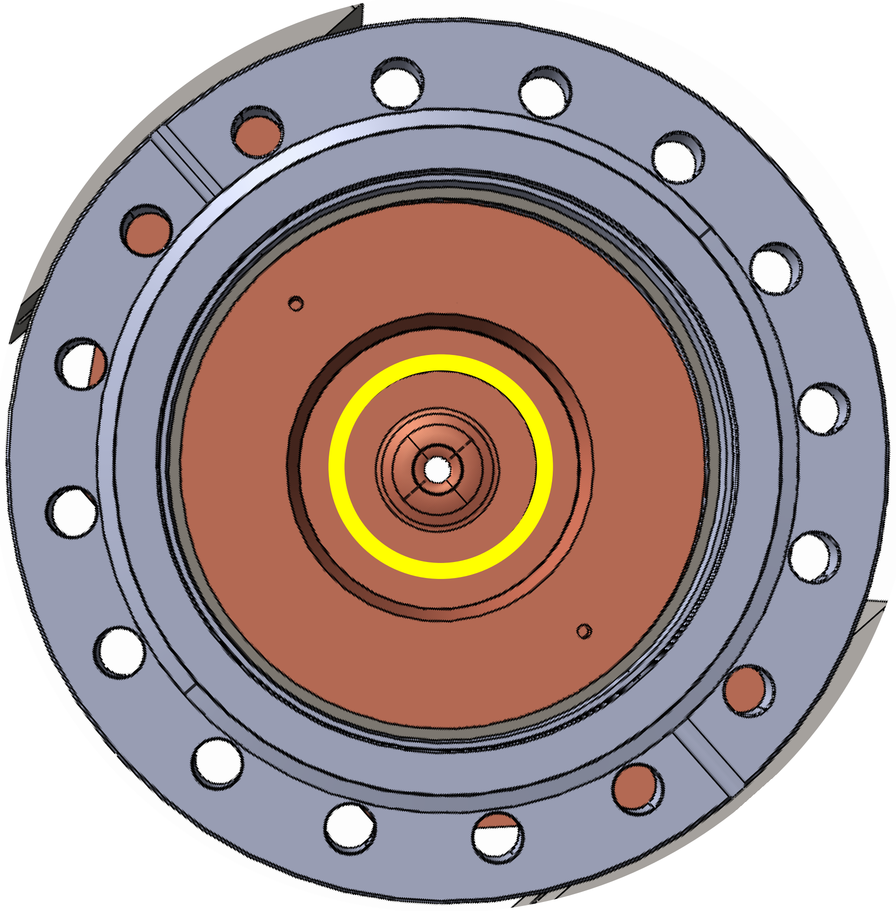

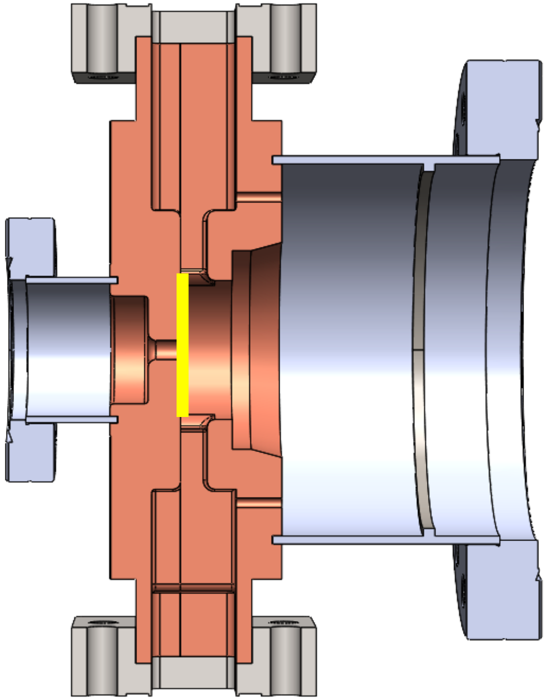

4. LLRF Measurements

- Low level RF measurements (LLRF) with vector network analyzer
- 295K resonance 6 MHz higher than intended and coupling lower
- Q0 = 4200 with no clamp, up to 7649 with firm but not aggressive clamp

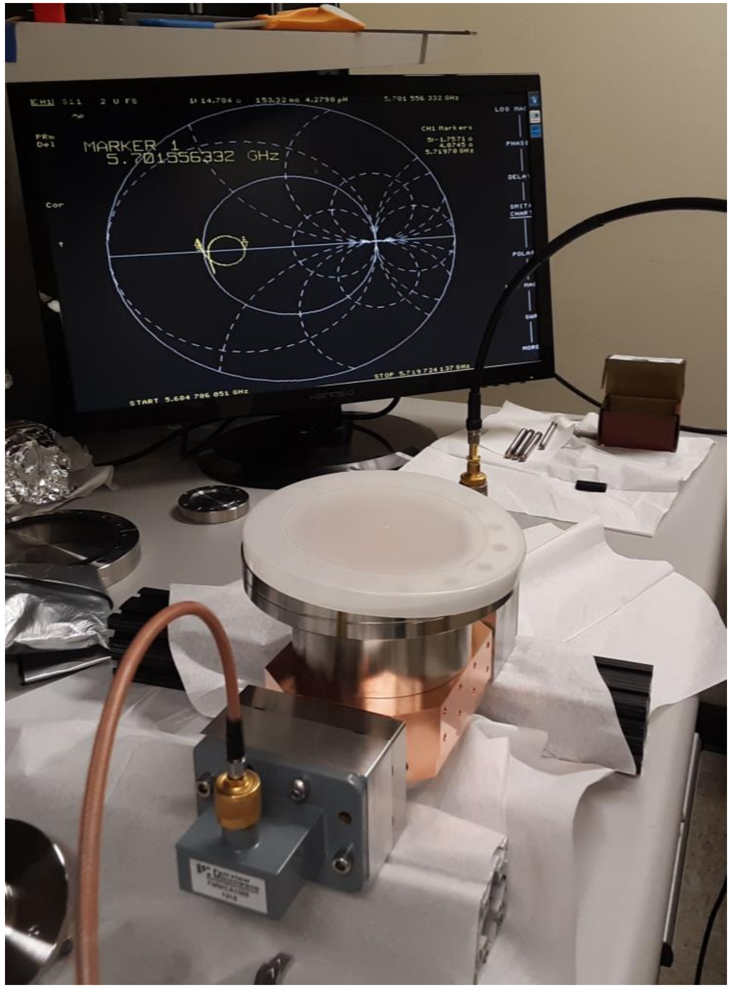

	Measurement	Design/Simulation
f0	5.701 GHz	5.695 GHz
β	0.52	0.7
QL	≈ 5000	5167
Q0 (partial clamp)	≈ 4600	-
Q0 (clamped)	7649	8579

4. Surface Sensitivity

- Attributed to presence of braze material
- Slater perturbation theory gives frequency change from small displacement of one surface
- LC circuit model of cavity $\omega^2 = \frac{1}{LC}$
- Removing small volume in vacuum cavity equiv. to adding small amount of material on surface, i.e. braze material
- 15 MHz bandwidth of klystron
- Set new working point for intermediate test between 90-100K

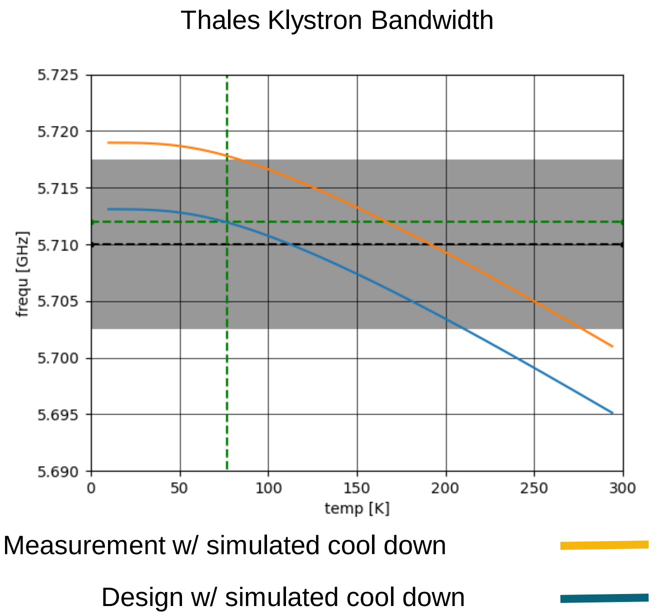

Parameter	100K
Launch field	120 MV/m
Frequency	5.711 GHz
β	3.1
Q0	18000
Filling time	0.25 us
RF Power requirement	0.56 MW
Energy deposition	0.22 J/pulse

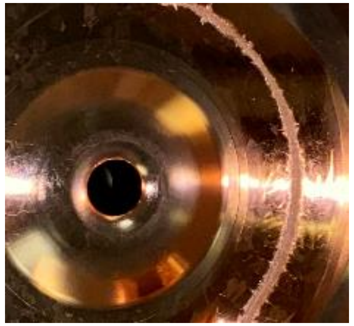

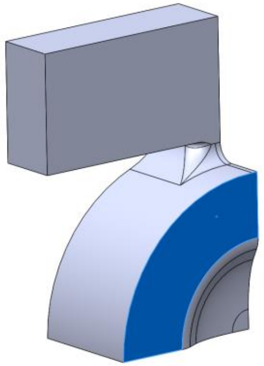

area $[\mathrm{mm}^2]$
720

$$\Delta f_i = \Delta s_i \frac{f_0}{4U} \int_{S_i} \left(\mu \left|H_0\right|^2 - \epsilon \left|E_0\right|^2\right) dS$$

tolerance $[\mu\mathrm{m}]$	detuning $[\mathrm{MHz}]$
5	0.648

5. Backplane Modifications

- Removal of material on backplane in high H, low E area on next backplane can shift resonance back into bandwidth

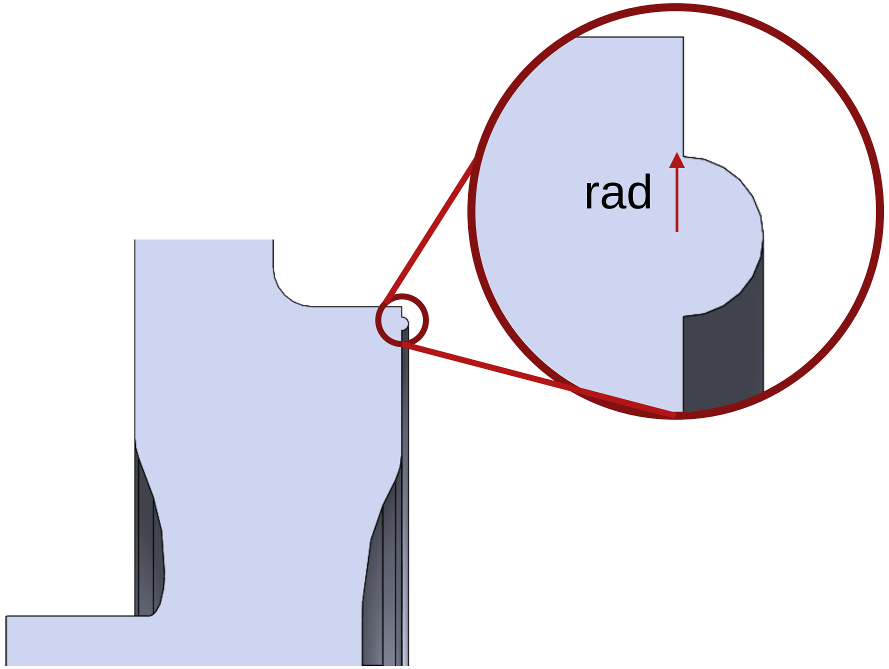

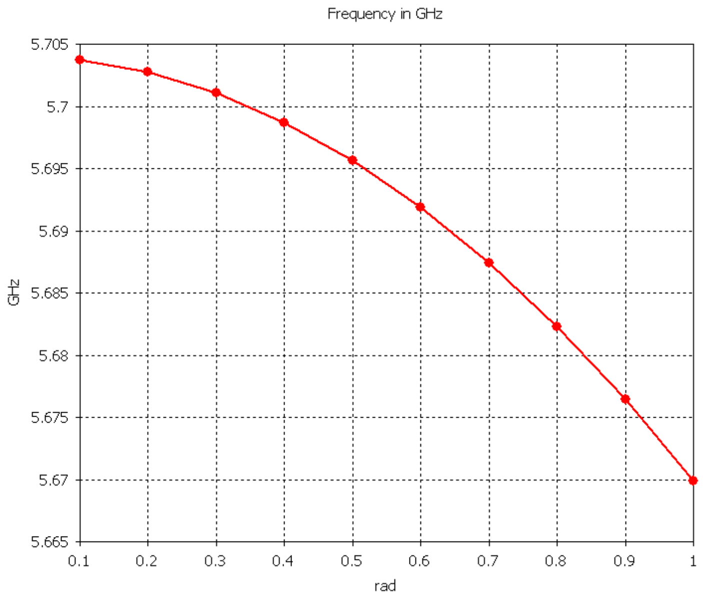

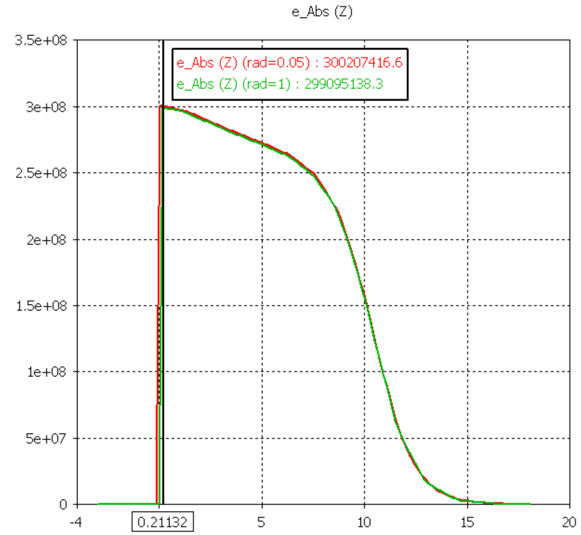

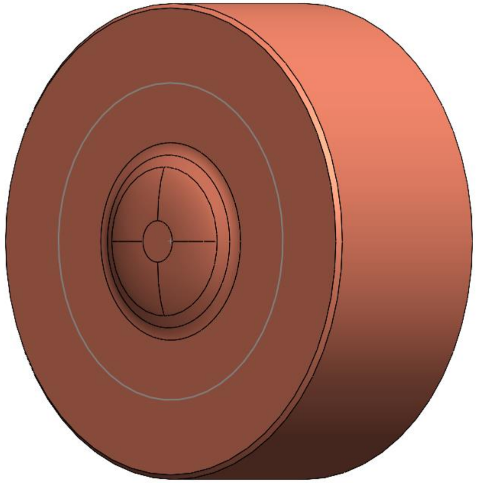

5. Testing Goals

1. C-band pillbox surface resistivity
2. CYBORG infrastructure: vacuum, cooldown, and temperature tuning
3. CYBORG cryo copper dark current (demountable backplane)
4. CYBORG cryo copper dark current (demountable backplane + copper plug)
5. CYBORG cryo copper photoemission
6. C-band breakdown tests
7. CYBORG semiconductor cathode emission

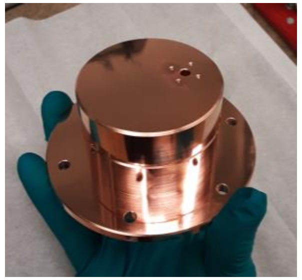

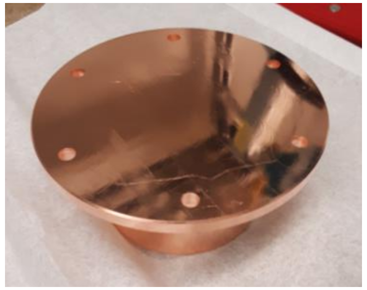

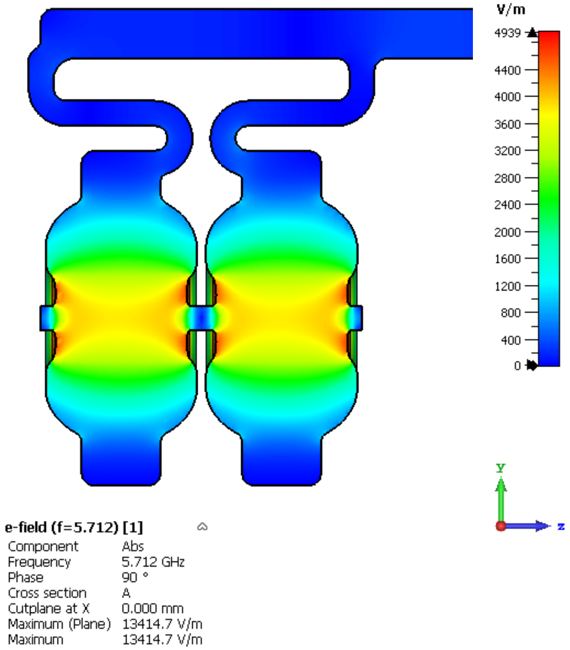

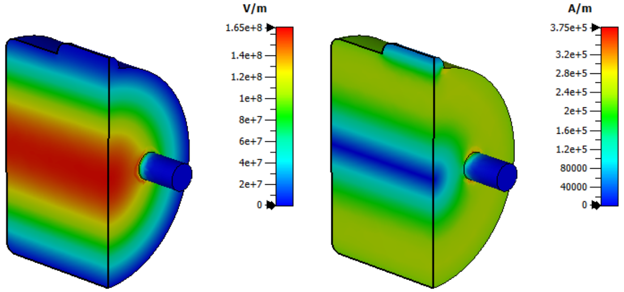

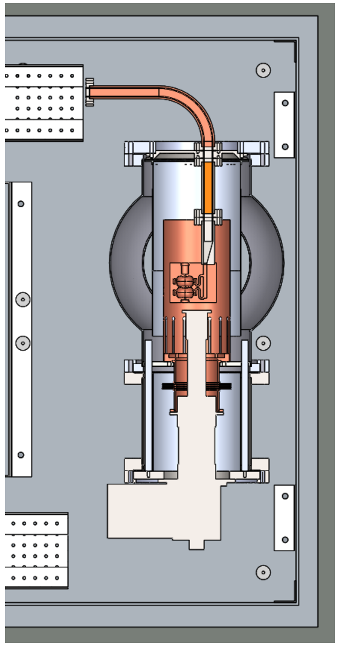

Conclusions

1. High gradient cryogenic test bed for cathode studies has been designed at under construction
2. Many future measurements planned (temperature dependent dark current etc.)
3. Continually maturing understanding of complex physics of breakdown necessary for increasing robustness of photoguns for precise brightness preserving cathode measurements

Additional References

- D. Dowell and J. Schmerge, Phys. Rev. ST Accel. Beams 12, 074201 (2009).
- M. C. Divall, E. Prat, S. Bettoni, C. Vicario, A. Trisorio, T. Schietinger, and C. P. Hauri, Phys. Rev. ST Accel. Beams 18, 033401 (2015).
- T. Vecchione, Proceedings of FEL2013 (JACOW, 2013), TUPSO83.
- J. Feng, J. Nasiatka, W. Wan, S. Karkare, J. Smedley, and H. A. Padmore, Appl. Phys. Lett. 107, 134101 (2015).
- L. Cultrera, I. Bazarov, A. Bartnik, B. Dunham, S. Karkare, R. Merluzzi, and M. Nichols, Appl. Phys. Lett. 99, 152110 (2011).
- L. Cultrera, S. Karkare, B. Lillard, A. Bartnik, I. Bazarov, B. Dunham, W. Schaff, and K. Smolenski, Appl. Phys. Lett. 103, 103504 (2013).
- G. S. Gevorkyan, S. Karkare, S. Emamian, I. V. Bazarov, and H. A. Padmore,Phys. Rev. Accel. Beams, vol. 21,p. 093 401, 9 Sep. 2018.
- I. Bazarov et al., Phys. Rev. Lett. 102, 104801 (2009)
- J.B. Rosenzweig, A. Cahill, B. Carlsten et al.Nuclear Inst. and Methods in Physics Research, A 909 (2018) 224–228
- D. H. Dowell and J. F. Schmerge, Phys.Rev. ST Accel. Beams, vol. 12, p. 074 201, 7 Jul. 2009.
- J. Maxson, L. Cultrera, C. Gulliford, and I. Bazarov, Applied Physics Letters, vol. 106, no. 23,p. 234 102, 2015
- H. Lee, X. Liu, L. Cultrera, B. Dunham, V. O. Kostroun, and I. V. Bazarov Rev. Sci. Instrum. 89, 083303 (2018).
- J B Rosenzweig et al 2020 New J. Phys. 22 093067
- G. E. Lawler, A. Fukasawa, N. Majernik, M. Yadav, A. Suraj, and J. B. Rosenzweig, “Rf testbed for cryogenic photoemission studies”, presented at the 12th Int. Particle Accelerator Conf. (IPAC’21), Campinas, Brazil, May 2021, paper WEPAB096